Journal of Ovonic Research Vol. 21, No. 3, May - June 2025, p. 365 - 376

Efficient photocatalytic degradation of 4-nitrophenol using titanium dioxide NpS obtained by sol gel process

E. Palma-Soto, C. Rodríguez, A. Dominguez Chicas[a], A. Carrillo- Castillo [*]
Institute of Engineering and Technology, Universidad Autónoma de Ciudad Juárez. Cd. Juárez Chihuahua. CP 32310, México

This research is related to the synthesis of titanium dioxide nanoparticles (NpS TiO_2) by the sol-gel method and its use as the solid interface to degradate 4-Nitrophenol (4-NP), an organic contaminant. Morphological, optical, and chemical characterization of the nanomaterial was carried out. The TiO_2 photocatalytic activity was determined, using an initial concentration of 19.62 ppm of 4-NP, after 5 hours of reaction, it was possible to degrade 47.44 % of the 4-NP, the TOC decreased by 30% and the pH had a variation from 5.93 to 4.2. Based on the results, the degradation route for the 4-NP was determined.

(Received March 10, 2025; Accepted June 16, 2025)

Keywords: Titanium dioxide nanoparticles, 4-Nitrophenol, Photocatalytic degradation, Sol gel process

1. Introduction

Nowadays, pollution in wastewater discharges is a global problem due to population growth, agricultural activities, industrial development and technology advances [1]. Some of these wastewater discharges contain organic pollutants with a very stable and recalcitrant aromatic chemical structure [2]. 4-Nitrophenol (4-NP) or p-nitro phenol is an aromatic nitro compound where the hydroxyl group (OH) is in the opposite position to the nitro group (see Figure 1) [3]. 4-NP is used as an intermediary during the production of petrochemical materials, pesticides, herbicides, pharmaceuticals, plastics and steelworks [4]. Additionally, this chemical compound is among the list of priority contaminants of the United States Environmental Protection Agency (USEPA) due to its high solubility and stability in water [5] and its high toxicity for humans, causing affectation in the nervous system, cardiovascular system, bone marrow through skin absorption; in fact, 4-NP is a carcinogenic substance [6]. The contaminant is very soluble in water so it cannot be removed by conventional wastewater treatment processes and it is necessary to apply the advanced oxidation process through heterogeneous photocatalysis, which is a process based on irradiating a semiconductor as metallic oxides such as Titanium dioxide (TiO_2), Zinc oxide (ZnO) and Cupper oxide (CuO); or chalcogenides such as Cadmium sulfide (CdS), Copper sulfide (CuS), Bismute sulfide (Bi_2S_3) and Zinc sulfide (ZnS). For instance. Mostafa et al. carried out the degradation of 4-NP with thin ZnO/CdO films. The CdO wasn't efficient to degrade the contaminant, due its high hole-electron recombination, but in combination with ZnO, the 4-NP degradation was achieved in 200 min [7]. Jiang et al. experimented with Bi_2S_3 and carbon, adding sodium borohidride as the reducing agent, obtaining the degradation of 500 ppm of 4-Np in one hour. The authors observed that the reducing agent addition to the solution was required, otherwise the material by itself was unneficcient to degradate the 4-NP [3]. On the other hand, Azam Khan used CdS in nanosheets and nanotubes to transform the 4-NP contaminant into the non-contaminant 4-AP (4-Aminophenol) [8]. Based on Khan results [8], Tong y et al. added silicon (Si)-hematite (Fe_2O_3) to CdS, obtaining the total degradation of 4-NP in 120 min [9]. In another research, Muersha et al. experimented with the photocatalytic degradation of 4-NP using the bismuth, titanium, zinc, and zirconium metallic oxides. A 30% of the initial concentration of TiO_2 was removed in 90 min [10].

[*] Corresponding author: amanda.carrillo@uacj.mx
https://doi.org/10.15251/JOR.2025.213.365

Molinari et al. used TiO_2 with light to generate the electron/hole pairs for the oxidation/reduction of the organic contaminant [11].

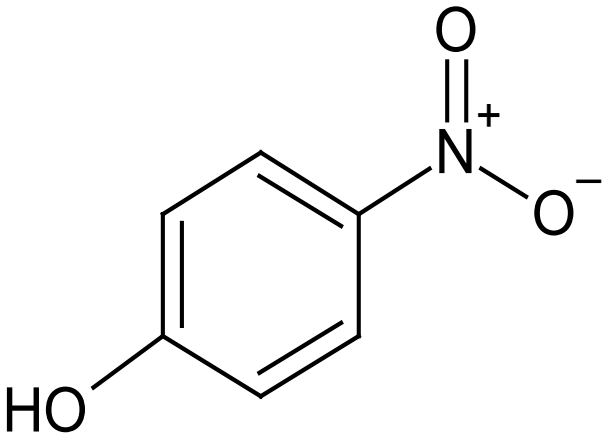

Fig. 1. 4-NP molecule.

Nanoparticles of titanium dioxide (TiO_2) were used in this research. This material is an inorganic n-type semiconductor that absorbs electromagnetic radiation in the ultraviolet region (UV,>400 nm) [12] having an energy gap band of 3.2 eV in the rutile phase and 3.0 eV in the anatase phase [13], where the anatase phase is the one with the highest photocatalytic activity [14]. Advantages of the material is its low cost, its photo-corrosion resistance, and its chemical inert and non-toxic properties [15]. For the synthesis of the TiO_2 nanoparticles, the microwave-assisted sol-gel method was used [16]; once the material was obtained, it was used as an interface for heterogeneous photocatalysis in a perfect mixing Slurry reactor. During the photocatalysis, several processes occur, including the adsorption and desorption of the persistent organic contaminant, generation of the electron-hole pairs, and chemical degradation reactions to transform the molecule of the contaminant until it is completely mineralized [17].

2. Experimental details

2.1. Materials

The following reagents were used to prepare the TiO_2 nanoparticles: titanium isopropoxide IV ($C_{12}H_{28}O_4Ti$, 97%, provided by Sigma-Aldrich, Toluca, México), isopropanol (C_3H_8O, 99.8%, provided by Fermont, Nuevo León, México) and etahnol (C_2H_5OH, 99.5%, provided by CTR, Nuevo León, México). To degrade the pollutant by heterogeneous photocatalysis, the organic pollutant 4-Nitrophenol ($O_2NC_6H_4OH$, provided Sigma-Aldrich brand, Madrid Spain) was used, as well as a slurry mixing reactor PYREX of 1 L surrounded by six UV lamps (PHILIPS brand, Black Light Blue UV-A model, 15 W) and four fluorescent lamps (PHILIPS brand, Day-light model, 15 W).

2.2. Preparation of the TiO_2 nanoparticles

The microwave-assisted sol-gel method was carried out, following the Mota-González methodology [16], for the synthesis of the TiO_2 nanoparticles. According to the methodology, 2.72 g of titanium isoproxide were poured into 40 ml of isopropanol, and leaving in agitation at 700 rpm for 1 minute at 80 °C, after one minute 0.52 ml of deionized water and 1 ml of isopropanol were added to shake them at 700 rpm for one minute at 80 °C. After one minute it was left in precipitation for 24 hours, after which time the solution was transformed into two phases (sol-gel), which was removed from the supernatant with a pipette.

To dry the solution, a microwave was used for 15 min, using at intervals of 5 sec of drying for 60 sec of resting outside the microwave. After drying, the nanoparticles were crushed in a mortar and then washed with deionized water.

2.3. Preparation of photocatalytic activity with photoreactor

For the degradation of 4-NP, the three-phase Slurry perfect mix reactor was used to be irradiated by 10 lamps; 6 UV lamps of 15 W and 4 fluorescent lamps of 15 W, where 0.5 g of TiO_2 catalyst was used in nano particles at a concentration of 19.62 ppm in milli Q deionized water.

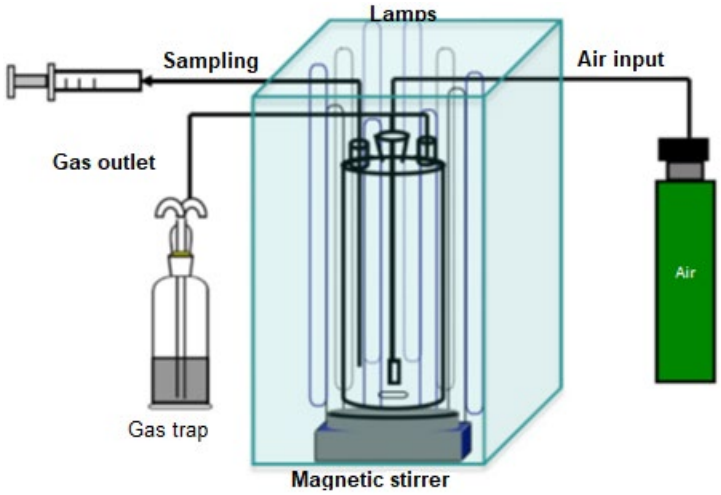

Fig. 2. Three-phase perfect mix Slurry reactor [18].

The three-phase reactor (see figure 2) is made up of a gas inlet O_2 where it is used as an oxidizer causing bubbling during the reaction process with the catalyst, TiO_2 in suspension, and a second outlet (gas trap) and a third outlet to collect the sample at certain times [19]

2.4. Characterization of TiO_2

Optical absorption measurements were made with a Jeneway 6850 UV/visible spectrophotometer (Sapulpa, OK, USA). The morphology and chemical composition of the materials were characterized with a Hitachi SU5000 scanning electron microscope (Hitachi, Tokyo, Japan) at a voltage of 15,000 V. The crystal structure of the materials was examined with an X-ray diffractometer using a PANalytical US, (Malvern, UK) with a CuK source, operated at 35,000 V and 23 Ma, with scans of 2θ in a range of 10 to 80 º. A transmission electron microscope (TEM) brand JEM model 2100 F (Tokio, Japón) operating at a resolution of 10 nm, 200 kV acceleration voltage and 1 Pa was used to confirm the crystalline characteristics and phases. N_2 adsorption and desorption isotherms were performed in a Micrometities model ASAP 2420 equipment (Georgia, US), with an adsorption of N_2 at 77.3 K (BET method). In thermogravimetry, a TA model SDT-Q600 (New Castle, US) was handled, operating from 0 °C-700 °C; 10 °C/min; N_2 and for the contact angle a Kruss microscope model DSA 30 (Madrid, Spain) was used.

2.5. Photocatalytic degradation of 4-Np

The photocatalytic activity of the TiO_2 nanoparticles suspended on the 4-NP was through a perfect mix reactor type Slurry, where it was irradiated at 39.36 W/m^2 by 10 lamps (6 UV lamps of 15 W and 4 fluorescent lamps of 15 W), preparing a solution in a 1 L of milli Q water at a concentration of 19.62 ppm of 4-NP and stirring it at 1,000 rpm for 2 hours at a temperature between 25 and 30 °C. Samples of this solution were extracted at 0 min, 15 min, 30 min, 45 min, 60 min, 90 min, 120 min, 180 min, 240 min and 300 min to analyze the photocatalytic process. The results were also analyzed by a SHIMADZU Total Organic Carbon (TOC) equipment model TOC-V CSH (Kyoto, Japan), an AZURA high performance liquid chromatograph (HPLC) HPLC Plus (Berlin,

Germany), a Metrohm Ion Chromatography (IC) model 883 Basic IC Plus (Herisau, Switzerland), and a CRISON model GLP22 potentiometer (Bilbao, Spain).

3. Results and discussions

3.1. Characterization of TiO_2 nanoparticles

3.1.1. Optical characterization

Figure 3 shows the absorption spectrum of TiO_2 nanoparticles; it shows absorption in the UV region at the wavelength of about 312 nm [20], which means that the photons are required at that wavelength and with a bandgap energy of 3.9 eV obtained by the Tauc method [21]. In order to excite the material and generate oxidizing radicals, compared to other authors such as Manmohan Lal and collaborators, the TiO_2 was subject to heat treatment to lower the bandgap energy; the values were similar since they use the sol-gel method synthesis [22]. The material was irradiated with UV lamps looking for the wavelength required to be able to emit photons by the 4-NP molecule. Naraginti obtained an absorption edge between 300 and 350 nm and used a 200 W tungsten lamp, deducing a higher irradiation power is required to generate the oxidizing radicals and therefore completely degrade the 4-NP [23].

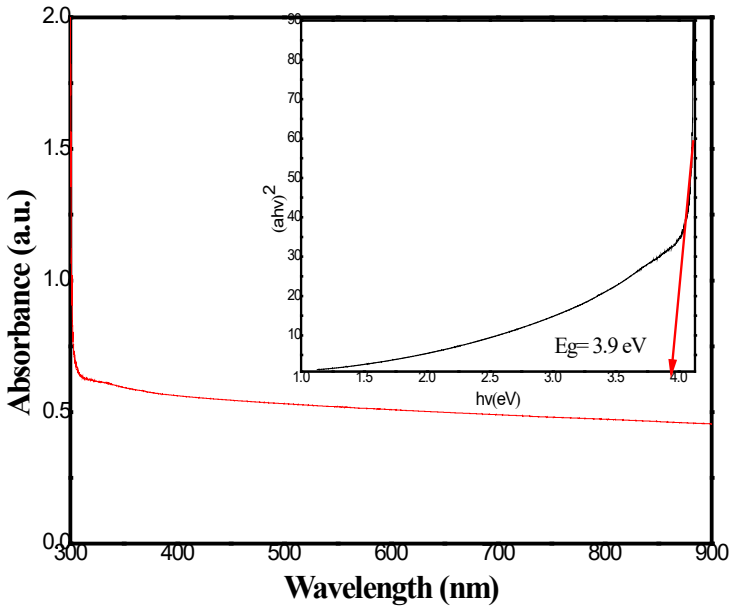

Fig. 3. Absorption of TiO_2 nanoparticles and Band gap of TiO_2 nanoparticles [24].

3.1.2. Morphology of TiO_2 nanoparticles

The morphology of the TiO_2 nanoparticles at 15 KX in Figure 4 is shown spherically and agglomerated, so this could affect the generation of photoactive radicals and could result in a longer degradation time of the contaminants [25]. Strbaca and collaborators found the same agglomeration of the TiO_2 nanoparticles and a size of approximately 100 nm [26].

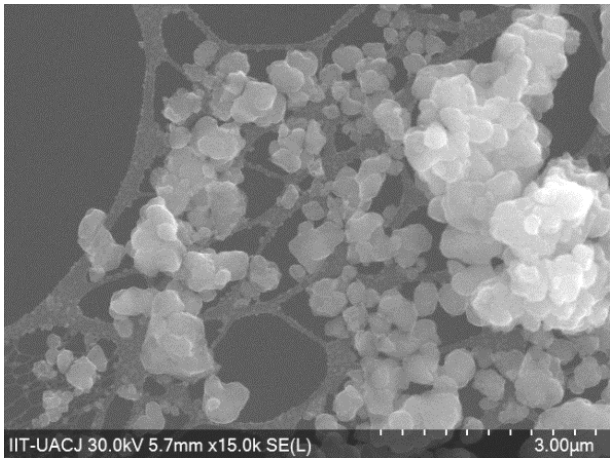

Fig. 4. SEM micrograph of TiO_2 nanoparticles [20].

3.1.3. Elemental chemical characterization of TiO_2 nanoparticles

Figure 5 shows the chemical composition of the TiO_2 nanoparticles, where there is the presence of Ti (Titanium) and O (Oxygen), elements desired for the confirmation of the catalyst.

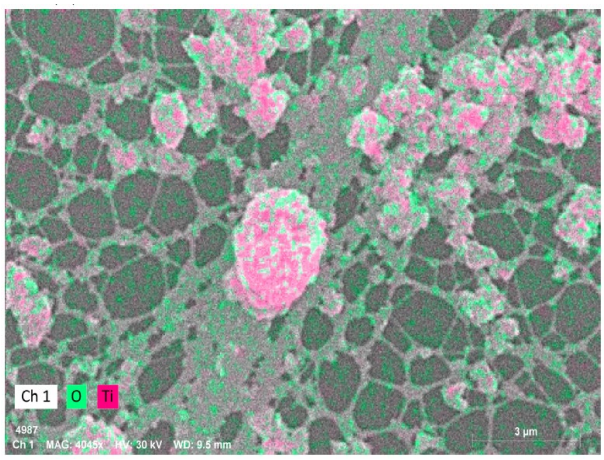

Fig. 5. Elemental chemical mapping of TiO_2.

3.1.4. X-ray diffraction of TiO_2 nanoparticles

Figure 6 shows the X-ray diffractogram, with the characteristic peak of TiO_2 nanoparticles$_2$ located in the crystallographic plane of the anatase phase (1 0 1), corresponding to the tetragonal structure [15][27]. This structure corresponds to the reference code 01-089-4921 of the X'Pert HighScore Plus computer program [25]. The characteristic peak of the rutile phase of TiO_2 is located at the 27° position, corresponding to the crystallographic plane (1 1 0) [28]. The structure corresponds to the reference code 01-076-0318 of the computer program previously mentioned. Moeini and cols. presented an immobilized TiO_2 film containing both phases with the characteristic peaks of the material (rutile and anatase); with these phases they managed to degrade 4-NP in 5 hours [29].

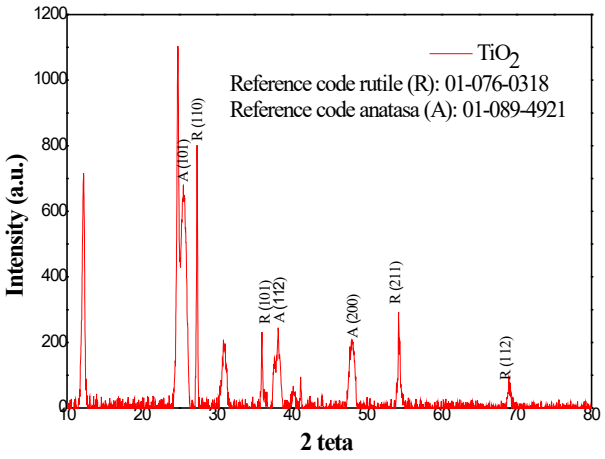

Fig. 6. Diffractogram of TiO2 nanoparticles [16].

3.1.5. Microstructural transmission electron microscope (TEM)

Figure 7 A) confirms the agglomeration of the TiO_2 nanoparticles and their spherical morphology as well as the SEM images. Figure 7 B) shows a polycrystalline material with small crystal lattices in different directions, in addition to an abundant agglomerate of the nanomaterial showing an irregular shape of the nanoparticles [30] [31]. Finally in Figure 7 C) it is possible to see the rings that are diffracted according to the crystallographic planes that are equivalent to the peaks of the diffractogram in Figure 5, represented by planes (101), (110), (101), (200) and (211), thus confirming the phases of TiO_2 [32].

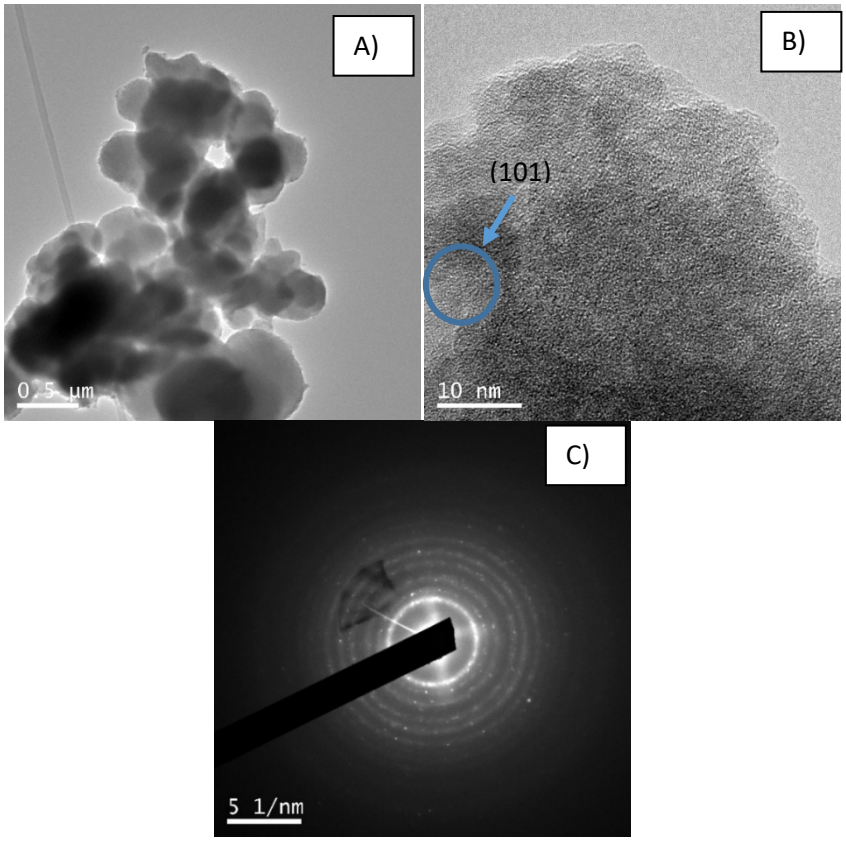

Fig. 7.- A) TEM image of TiO_2 nanoparticles, B) High-resolution TEM image of TiO_2 nanoparticles C) Debye-Scherrer rings of TiO_2 nanoparticles.

3.1.6. Gas adsorption technique for TiO_2

Figure 8 shows the graph of N_2 absorption and desorption isotherms for TiO_2 nanoparticles used to determine textural properties [33]. A IV type isotherm behavior according to the classification of the International Union of Pure and Applied Chemistry (IUPAC), which is associated with 2-50 nm mesoporous materials [33][34]. The pore size is associated with catalyst efficiency and is therefore considered to degrade the molecule of 4-NP with the pore size of TiO_2 (2.4297 nm) [35]. The hysteresis loop formed in the graph is associated with the typical capillary condensation of adsorption-desorption in the mesosporous of the material [36].

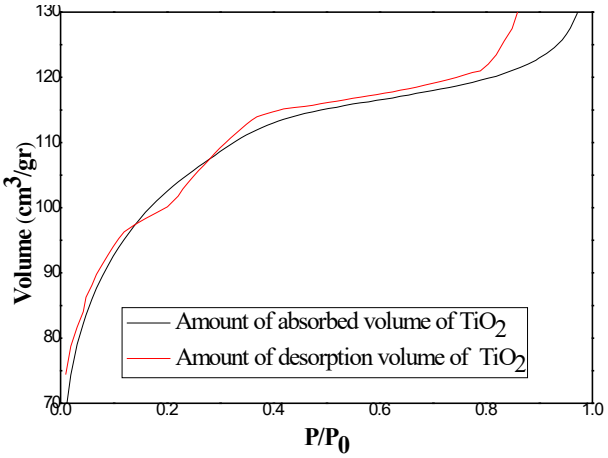

Fig. 8. Adsorption-desorption isotherm of N_2 of TiO_2.

With the Brunauer–Emmett–Teller (BET) technique, the surface area related to the volume of N_2 (adsorbate) adsorbed by the TiO_2 (adsorbent) was estimated as 335.0912 m2/g. Basically, the BET area represents the number of N_2 molecules needed to surround the TiO_2, thus the monolayer of the adsorbate on the photocatalytic material at constant pressure produces an equilibrium between the molecules, producing the isotherms. The pore size of the material is 2.4297 nm, classifying, based on this value, the photocatalytic material as mesoporous (2 nm – 50 nm in pore size) [37]. Finally, a pore volume value of 0.2035 m3/g was obtained. See Table 1 [38].

Table 1. BET area, size and pore volume of TiO_2 nanoparticles.

Catalyst	SBET	Pore Volume	Pore Size
TiO_2	335.0912 m^2/g	0.2035 m^3/g	2.4297 nm

Other researchers, such as Caudillo and collaborators, synthesized TiO_2 nanoparticles, obtaining pore sizes ranging from 2.1 nm to 9.3 nm; the researchers observed that Toluene degradation is more efficient when the largest pore size of the nanoparticles were used (9.3 nm) [39].

3.1.7. Thermogravimetry of TiO_2 nanoparticles

The thermogram in Figure 9 shows some areas of weight percentage loss as a function of temperature increase. The first stage of weight loss, from 30 °C to 125 °C, is attributed to the loss of adsorbed water molecules associated with hydrogen bonds and solvent evaporation [40]. In the second stage, from 125 °C to 250 °C the TiO_2 loses up to 25% of its weight due the combustion of organic compounds [41] and the phase change of anatase-rutile [42]. Afterwards, the TiO_2 is kept without material weight loss which means it is resistant to elevated temperatures. The third zone or stage, where weight percentage is lost, is called the final temperature because it reaches the maximum loss at 400 °C and is set at 800 °C [43].

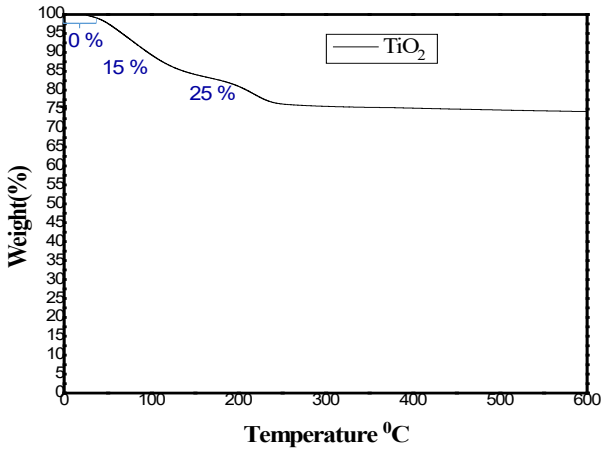

Fig. 9. Thermogram of TiO_2 nanoparticles.

3.2. Heterogeneous photocatalytic activity of 4-Nitrophenol using TiO_2 as a catalyst

The photocatalytic activity of TiO_2 nanoparticles on 4-NP was evaluated for total organic carbon (TOC) and total concentration of the organic pollutant after 5 hours of reaction (see Figure 10).

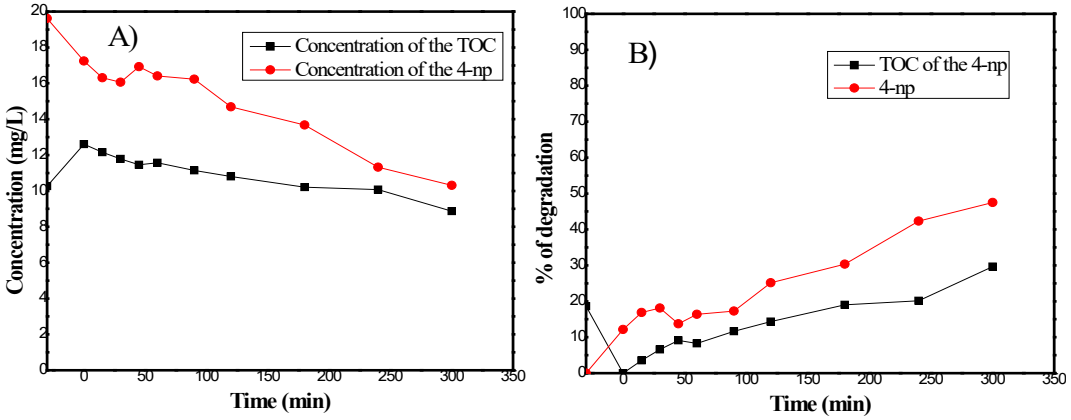

Fig. 10. Degradation graph of 4-NP, A) Degradation of the 4-NP in ppm B) Degradation of the 4-NP in percentage.

The initial TOC was 12.61 ppm and an initial concentration of 19.62 ppm of 4-NP (see figure 10 A)), after 5 hours of reaction there was a decrease of 30% of TOC (8.87 ppm) and the total concentration decreased by 47.44 % (see figure 10 B)), shows degradation in percentage) leaving a concentration of 10.30 ppm. During the reaction time the 4-NP molecule was transformed into less polluting molecules, according to results from the ion chromatography and in an HPLC techniques [44].

Figure 11 shows the degradation route of 4-NP (1). where the first sample was extracted after 15 min, in that time the nitrogen dioxide (NO_2) molecule was detached from the original molecule, at the same time that the hydroxyl radicals (OH) were generated from the surface of TiO_2, these adhere to the benzene ring and depending on the position where they adhere they are called catechol (4), resorcinol (2), or hydroquinone (3) [45]. At 30 min of sample extraction, 1,2,4-trihydroxybenzene (5) was detected, where more OH radicals attack the aromatic ring while ammonia molecules (NH_4^+) are formed. At minute 45 of the reaction, a rupture of the benzene ring is shown forming the maleate (6) [46], The, after 90 min, more aliphatic acid chains such as acetic

acid (7) and oxalic acid (8) are formed [47]; it is for this reason that between minute 45 and 100 the pH of the solution is more acidic. As shown in Figure 12, the relationship of pH with the solution is associated with the generation of OH radicals which results in an oxidation of 4-NP [48].

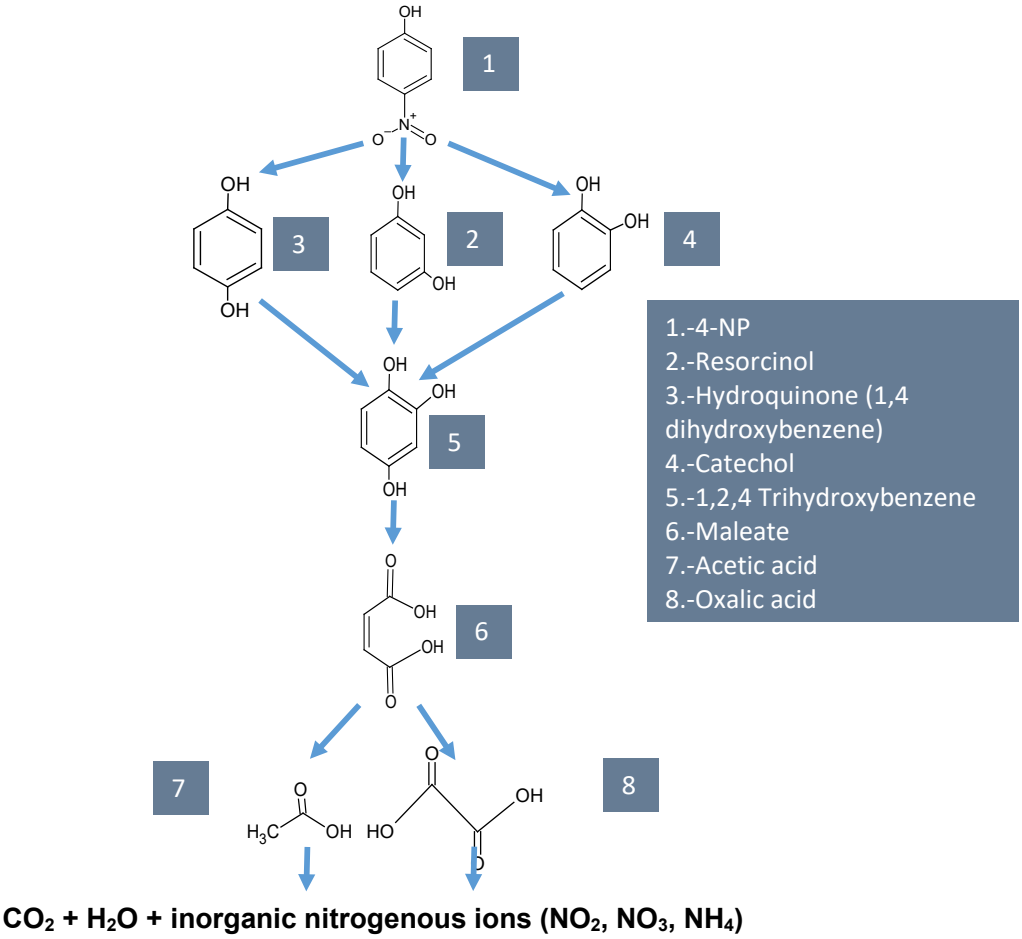

Fig. 11. Degradation pathway of 4-NP.

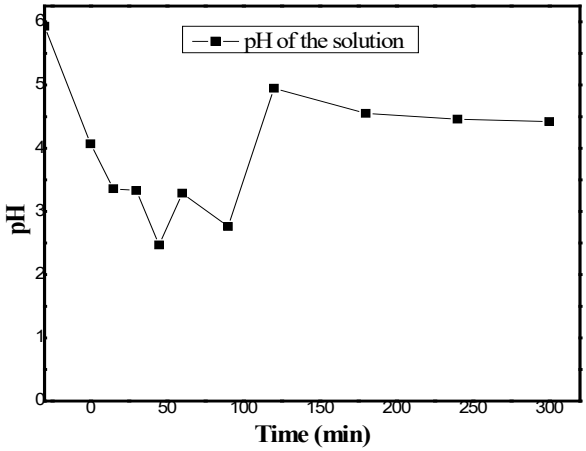

Fig. 12. pH of the 4-NP degradation solution.

The compounds formed in photooxidation cause acidification of the solution throughout the reaction, going from an initial pH of 5.93 to a final pH of 4.2, but lowers the pH to 2.47 in a reaction time of 45 min (see figure 12). Acidification destabilizes the catalysts, but TiO_2 is considered stable so it did not undergo any modification [49], Sood et al. used the same amount of catalyst (0.5 g of TiO_2) but at a lower concentration (10 ppm), obtaining a degradation of 90% in 300 min [50]. Compared to these results, the TiO_2 catalyst synthesized in this research was less efficient but other characteristics of the catalyst were improved; for instance, obtaining the catalyst at low temperatures, a greater surface area, lower porosity, and the presence of the two phases anatase and rutile.

4. Conclusions

A stable material has been synthesized when TiO_2 is used as a photocatalyst in the degradation of the organic molecule 4-NP. TiO_2 has a spherical morphology with agglomerations, having two crystallographic phases (anatase phase and rutile phase), covers an area of 335.0912 m2/g, a pore volume of 0.2035 m3/g and a pore size of 2.4297 nm, and can be excited at a wavelength of 315 nm with a bandgap energy of 3.9 eV.

After 300 min, the TiO_2 nanoparticles degraded to 4-NP by 47.44%, having an initial concentration of 19.62 ppm and a final concentration of 10.30 ppm was obtained. During the reaction, the 4-NP molecule was transformed into acetic acid and oxalic acid, pollutants with less impact on the environment, generating a pH change in the solution due to the aliphatic acid chains and nitrogenous ions formed.

References

[1] J. Schneider et al., Chemical Reviews, vol. 114, no. 19, pp. 9919-9986, 2014; https://doi.org/10.1021/cr5001892

[2] A. Di, E. García-lópez, G. Marcì, L. Palmisano, Journal of Hazardous Materials, vol. 211-212, pp. 3-29, 2012; https://doi.org/10.1016/j.jhazmat.2011.11.050

[3] J. Jiang et al., Colloids and Interface Science Communications, vol. 51, no. October, p. 100678, 2022; https://doi.org/10.1016/j.colcom.2022.100678

[4] E. Y. Danish, H. M. Marwani, M. A. Alhazmi, Desalination and Water Treatment, vol. 67, pp. 239-246, 2017; https://doi.org/10.5004/dwt.2017.20362

[5] Z. Min Tang, L. Zhang, J. Jing Du, L. Jian Xu, Transactions of Nonferrous Metals Society of China (English Edition), vol. 32, no. 6, pp. 1994-2002, 2022; https://doi.org/10.1016/S1003-6326(22)65925-9

[6] F. Amarloo, R. Zhiani, A. Motavalizadehkakhky, M. Hosseiny, J. Mehrzad, Desalination and Water Treatment, vol. 313, pp. 116-124, 2023; https://doi.org/10.5004/dwt.2023.30081

[7] A. M. Mostafa, E. A. Mwafy, Journal of Molecular Structure, vol. 1221, p. 128872, 2020; https://doi.org/10.1016/j.molstruc.2020.128872

[8] A. Khan et al., Inorganic Chemistry Communications, vol. 79, pp. 99-103, 2017; https://doi.org/10.1016/j.inoche.2017.03.033

[9] M. Tong, D. Sun, R. Zhang, H. Liu, R. Chen, Journal of Alloys and Compounds, vol. 862, p. 158271, 2021; https://doi.org/10.1016/j.jallcom.2020.158271

[10] W. Muersha, G. S. Pozan Soylu, Journal of Molecular Structure, vol. 1174, pp. 96-102, 2018; https://doi.org/10.1016/j.molstruc.2018.07.034

[11] R. Molinari, C. Lavorato, P. Argurio, Catalysis Today, vol. 281, pp. 144-164, 2017; https://doi.org/10.1016/j.cattod.2016.06.047

[12] W. Liu, T. He, Y. Wang, G. Ning, Z. Xu, X. Chen, Synergistic adsorption - photocatalytic degradation effect and norfloxacin mechanism of ZnO / ZnS @ BC under UV - light irradiation, pp. 1-12, 2020; https://doi.org/10.1038/s41598-020-68517-x

[13] Z. Youssef et al., Dyes and Pigments, vol. 159, no. May, pp. 49-71, 2018; https://doi.org/10.1016/j.dyepig.2018.06.002

[14] Y. Luo et al., Materials Chemistry and Physics, vol. 258, no. August 2020, p. 123884, 2021; https://doi.org/10.1016/j.matchemphys.2020.123884

[15] A. H. Shah, M. A. Rather, Materials Today: Proceedings, 2021, vol. 44, pp. 482-488; https://doi.org/10.1016/j.matpr.2020.10.199

[16] M. Mota-gonzález, H. Hernández-carrillo, M. Alaniz-hernandez, TiO 2 obtenido por el proceso sol gel asistido con microondas, vol. 3, no. 1, pp. 1-4, 2018; https://doi.org/10.69681/lajae.v3i1.14

[17] F. Shokry, M. El-Gedawy, S. A. Nosier, M. H. Abdel-Aziz, Results in Chemistry, vol. 13, no. September 2024, p. 101980, 2025; https://doi.org/10.1016/j.rechem.2024.101980

[18] Tolosana Moranchel Alvaro, Tesis Doctoral Álvaro Tolosana Moranchel, 2019.

[19] E. Diaz et al., Catalysis Today, vol. 266, pp. 168-174, 2016; https://doi.org/10.1016/j.cattod.2015.08.013

[20] E. Palma-Soto, M. de La Luz Mota-González, P. A. Luque-Morales, A. Carrillo-Castillo, Chalcogenide Letters, vol. 18, no. 2, pp. 47-58, 2021; https://doi.org/10.15251/CL.2021.182.47

[21] D. Komaraiah, P. Madhukar, Y. Vijayakumar, M. V. Ramana Reddy, R. Sayanna, Materials Today: Proceedings, vol. 3, no. 10, pp. 3770-3778, 2016; https://doi.org/10.1016/j.matpr.2016.11.026

[22] M. Lal, P. Sharma, C. Ram, Optik, vol. 241, Sep. 2021; https://doi.org/10.1016/j.ijleo.2021.166934

[23] S. Naraginti, F. B. Stephen, A. Radhakrishnan, A. Sivakumar, Spectrochimica Acta - Part A: Molecular and Biomolecular Spectroscopy, vol. 135, pp. 814-819, 2015; https://doi.org/10.1016/j.saa.2014.07.070

[24] E. Palma-soto, M. D. E. L. A. L. U. Z. Mota-González, Determination of photocatalytic activity for the system : CdS Chemical bath deposited thin films coated with TiO 2 NPs, vol. 18, no. 2, pp. 47-58, 2021; https://doi.org/10.15251/CL.2021.182.47

[25] J. A. Mendoza, D. H. Lee, J. Kang, Chemosphere, vol. 182, pp. 539-546, 2017; https://doi.org/10.1016/j.chemosphere.2017.05.069

[26] D. Štrbac et al., Process Safety and Environmental Protection, vol. 113, pp. 174-183, 2018; https://doi.org/10.1016/j.psep.2017.10.007

[27] M. Tahir, N. S. Amin, Applied Catalysis A, General, vol. 467, pp. 483-496, 2013; https://doi.org/10.1016/j.apcata.2013.07.056

[28] G. Jayanthi Kalaivani, S. K. Suja, Carbohydrate Polymers, vol. 143, pp. 51-60, 2016; https://doi.org/10.1016/j.carbpol.2016.01.054

[29] S. Moeini Najafabadi, F. Rashidi, M. Rezaei, Chemical Engineering and Processing - Process Intensification, vol. 146, p. 107668, 2019; https://doi.org/10.1016/j.cep.2019.107668

[30] A. Mishra, A. Mehta, S. Basu, Journal of Environmental Chemical Engineering Clay supported TiO 2 nanoparticles for photocatalytic degradation of environmental pollutants : A review, vol. 6, no. April, pp. 6088-6107, 2018; https://doi.org/10.1016/j.jece.2018.09.029

[31] H. Zou, M. Song, F. Yi, L. Bian, P. Liu, S. Zhang, Journal of Alloys and Compounds, vol. 680, pp. 54-59, 2016; https://doi.org/10.1016/j.jallcom.2016.04.094

[32] A. Bokare, M. Pai, A. A. Athawale, Solar Energy, vol. 91, pp. 111-119, 2013; https://doi.org/10.1016/j.solener.2013.02.005

[33] F. Wu et al., Applied Surface Science, vol. 358, pp. 425-435, 2015; https://doi.org/10.1016/j.apsusc.2015.08.161

[34] N. Yao, K. Lun Yeung, Chemical Engineering Journal, vol. 167, no. 1, pp. 13-21, 2011; https://doi.org/10.1016/j.cej.2010.11.061

[35] W. Dong et al., Applied Surface Science, vol. 349, pp. 279-286, 2015; https://doi.org/10.1016/j.apsusc.2015.04.207

[36] A. Magdziarz, J. C. Colmenares, O. Chernyayeva, D. Łomot, K. Sobczak, Journal of Molecular Catalysis A: Chemical, vol. 425, pp. 1-9, 2016; https://doi.org/10.1016/j.molcata.2016.09.021

[37] Q. Shen, J. Xue, H. Zhao, M. Shao, X. Liu, H. Jia, Journal of Alloys and Compounds, vol. 695, pp. 1080-1087, 2017; https://doi.org/10.1016/j.jallcom.2016.10.233

[38] C. Dong, J. Liu, M. Xing, J. Zhang, Research on Chemical Intermediates, vol. 44, no. 11, pp. 7079-7091, 2018; https://doi.org/10.1007/s11164-018-3543-5

[39] U. Caudillo-flores et al., Chemical Engineering Journal, vol. 299, pp. 393-402, 2016; https://doi.org/10.1016/j.cej.2016.04.090

[40] H. Zhu, R. Jiang, L. Xiao, L. Liu, C. Cao, G. Zeng, Applied Surface Science, vol. 273, pp. 661-669, 2013; https://doi.org/10.1016/j.apsusc.2013.02.106

[41] D. X. Martínez Vargas, J. Rivera De la Rosa, C. J. Lucio-Ortiz, A. Hernández-Ramirez, G. A. Flores-Escamilla, C. D. Garcia, Applied Catalysis B: Environmental, vol. 179, pp. 249-261, 2015; https://doi.org/10.1016/j.apcatb.2015.05.019

[42] E. Paradisi, P. J. Plaza-González, G. Baldi, J. M. Catalá-Civera, C. Leonelli, Materials Letters, vol. 338, no. January, pp. 0-4, 2023; https://doi.org/10.1016/j.matlet.2023.133975

[43] L. Alicia, R. Llamas, A. J. Azuara, J. M. M. Rosales, Adsorción del naranja de metilo en solución acuosa sobre hidróxidos dobles laminares, vol. 25, no. 3, pp. 25-34, 2015; https://doi.org/10.15174/au.2015.778

[44] A. Tolosana-moranchel, D. Ovejero, B. Barco, A. Bahamonde, E. Díaz, M. Faraldos, Journal of Environmental Chemical Engineering, vol. 7, no. 3, p. 103051, 2019; https://doi.org/10.1016/j.jece.2019.103051

[45] N. T. T. Van et al., Environmental Technology and Innovation, vol. 30, p. 103041, 2023.

[46] Z. Zhang et al., Journal of Electroanalytical Chemistry, vol. 895, no. April, p. 115493, 2021; https://doi.org/10.1016/j.jelechem.2021.115493

[47] C. S. D. Rodrigues, S. N. A. Aziz, M. F. R. Pereira, O. S. G. P. Soares, L. M. Madeira, Journal of Environmental Management, vol. 343, no. May, p. 118140, 2023; https://doi.org/10.1016/j.jenvman.2023.118140

[48] T. Li, Z. Zhao, Q. Wang, P. Xie, J. Ma, Water Research, vol. 105, pp. 479-486, 2016; https://doi.org/10.1016/j.watres.2016.09.019

[49] Y. Huo, X. Yang, J. Zhu, H. Li, Applied Catalysis B: Environmental, vol. 106, no. 1-2, pp. 69-75, 2011; https://doi.org/10.1016/j.apcatb.2011.05.006

[50] S. Sood, A. Umar, S. K. Mehta, S. K. Kansal, Journal of Colloid and Interface Science, vol. 450, pp. 213-223, 2015; https://doi.org/10.1016/j.jcis.2015.03.018